D5-47 35

1.2.3 OBSERVATIONS OF MESOSCALE VERTICAL VELOCITIES AROUND FRONTAL ZONES

T. S. Dennis, M. F. Larsen

Department of Physics
Clemson University
Clemson, South Carolina 29631

N87-10424

J. Rottger*

Arecibo Observatory
Box 995
Arecibo, Puerto Rico 00612

INTRODUCTION

We have analyzed vertical velocity and reflectivity data obtained with a VHF Doppler radar over a 15-day period in October and November of 1981 (DENNIS, 1985). Standard radiosonde data and surface observations have been used to locate two occluded fronts, two warm fronts, and a cold front that passed the radar site. These fronts are also evident in the radar reflectivity data.

Most studies of the vertical circulation patterns associated with mesoscale systems have used precipitation and cloud formations as tracers. Unlike other observational techniques, the VHF radar permits the continuous measurement of the three-dimensional air velocity vector in time and height from a fixed location. With the beam in a vertically pointing position, signals are scattered from turbulent variations in the refractive index with half the scale of the radar wavelength and by regions with sudden changes in the refractive index associated with horizontally stratified layers. Generally, the strongest echoes occur at the maximum in the vertical gradient of refractivity, usually at the base of a temperature inversion, such as the tropopause.

VHF radars can also be used to locate atmospheric fronts, which are characterized by static stability, large horizontal temperature gradients, large vorticities, and vertical wind shears (LARSEN and ROTTGER, 1982, 1983, 1984). Since these radars are not restricted to clear-air observations, they can provide the velocity field data needed to study wave motions associated with fronts and to compare the actual vertical circulation to theoretical predictions. These radars can provide data on the horizontal and vertical components of the wind with vertical resolution of approximately 150 to 300 meters and temporal resolution of about 1 minute.

DESCRIPTION OF THE DATA SET

The SOUSY VHF radar is located near Bad Lauterberg, West Germany, and is operated by the Max-Planck Institute. It is a pulsed coherent radar operating at a wavelength of 5.6 meters. From 1600 GMT on October 28 through 1400 GMT on November 12, 1981, the radar wind profiler was operated in the spaced antenna mode using 196 Yagi antennas for transmission and three arrays of 32 Yagi antennas for each reception. The spaced antenna technique uses vertically pointing transmitters and thus detects echoes with a higher signal-to-noise ratio than could be achieved with off-vertical beams. The applied average transmitter power for this experiment was 20 kW with a height resolution of

*On leave from Max-Planck-Institut fur Aeronomie, Katlenburg-Lindau, West Germany.

150 to 300 m and an effective antenna aperture of 2500 mB2. The height range is limited to 3.6 to 21.67 km due to the signal-to-noise levels. Approximately one minute is required for each profile, but the radar was not run continuously in order to reduce the amount of raw data. Throughout the period, data were taken for at least 12 minutes on the hour, but there were also two periods of continuous data taken so that five 12-minute averages per hour were available for a detailed view of approximately 30 hours beginning at 1600 GMT on October 28 and of approximately 24 hours beginning at 1500 GMT on November 4.

POTENTIAL TEMPERATURES AND RADAR REFLECTIVITIES

Potential temperatures and reflectivities are shown in Figures 1 and 2 with contours at 5-K and 3-dB intervals, respectively. The tropopause heights recorded by the radiosonde, represented as solid dots in each graph, agree with the levels indicated by the grouping of the potential temperature contours and by the higher reflectivity levels in these areas.

Frontal systems cause a packing in the potential temperature contour lines. The contours sloping downward from left to right represent warm fronts with upper-level effects occurring first while those sloping upward represent cold fronts. The use of radiosonde potential temperature contours only give the approximate location of frontal zones due to the poor time resolution. There are many unexplained deviations in the contours that may be the result of changes in the slopes of fronts or perhaps small fronts not established in the data analysis. By comparing the potential temperature contour groupings to breaks in the reflectivity contours, the location of frontal zones are more accurately established. The major disturbances include an occlusion, a warm front followed by a cold front, on October 29 and another occlusion on October 31; a warm front that arrives at the surface on November 3; a surface cold frontal passage on November 4; and a warm front that passed the surface on November 12. There are also two upper-level fronts that cause distinctive breaks in the reflectivity contours. The warm front on November 7 and 8

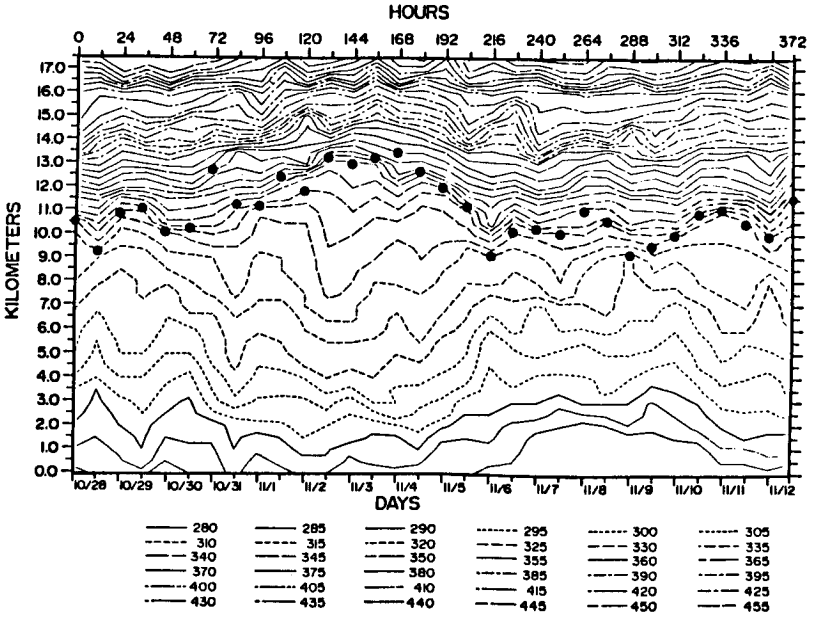

Figure 1. Potential temperature (K) with contours as indicated.

ORIGINAL PAGE IS
OF POOR QUALITY

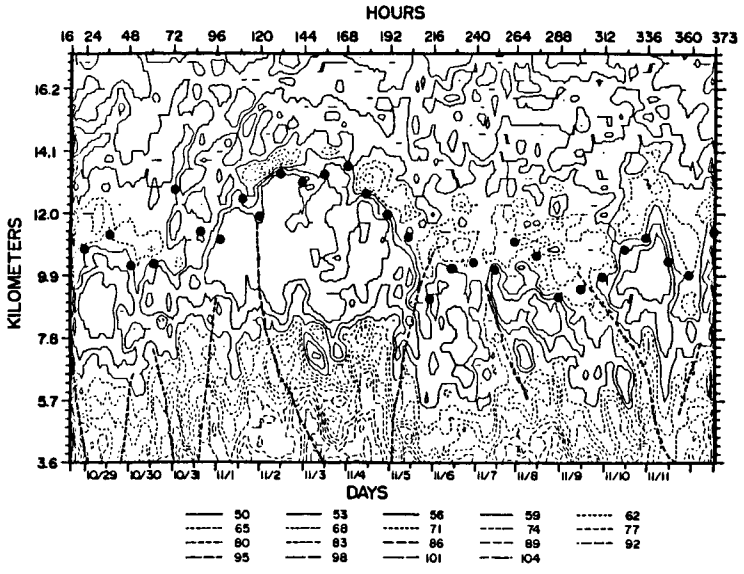

Figure 2. Radar reflectivity (dB) with contours as indicated.

stretches from 10 km down to 6 km, and the cold front on November 11 and 12 reaches up from 5 km to 8 km. These fronts have been sketched as dotted lines in Figure 2.

Beginning around October 30, the tropopause began to rise rapidly. There may even have been a separation of the lower tropopause as seen in the splitting of the potential temperature contour lines. The disturbance near the tropopause was present through November 4 and peaked around November 2. This phenomenon has all the characteristics of a tropopause fold, although the potential vorticity cross section will have to be calculated for confirmation.

VERTICAL VELOCITIES

The vertical velocities measured by the radar are contoured at 2-cm/s intervals with upward velocities graphed in Figure 3 and downward velocities graphed in Figure 4. The established fronts are drawn as dotted lines and the radiosonde tropopause levels are shown as solid dots. The most striking feature of these two graphs is the vertical stratification of the vertical velocities. Some regions are dominated by vertically stratified waves of upward velocities reaching to the top of the tropopause, while similar waves of downward velocity dominate other regions.

OCCLUSION

The occlusion on October 31 partially overlaps the less occluded front of October 29 and may cause variations in the normal occluded circulation patterns. There are waves of strong downward flow in the pockets between the warm and cold fronts, where a zone of rising air was expected to be found. The downward flow becomes more intense at lower levels in the occlusions with velocities reaching 26 cm/s at 3.6 km on October 29 and 40 cm/s at 4 km on October 31. A column of strong subsidence reaches 26 cm/s on October 30 between the two occluded fronts, which is expected of air beneath a cold frontal zone and beneath an approaching warm frontal zone.

ORIGINAL PAGE IS
OF POOR QUALITY

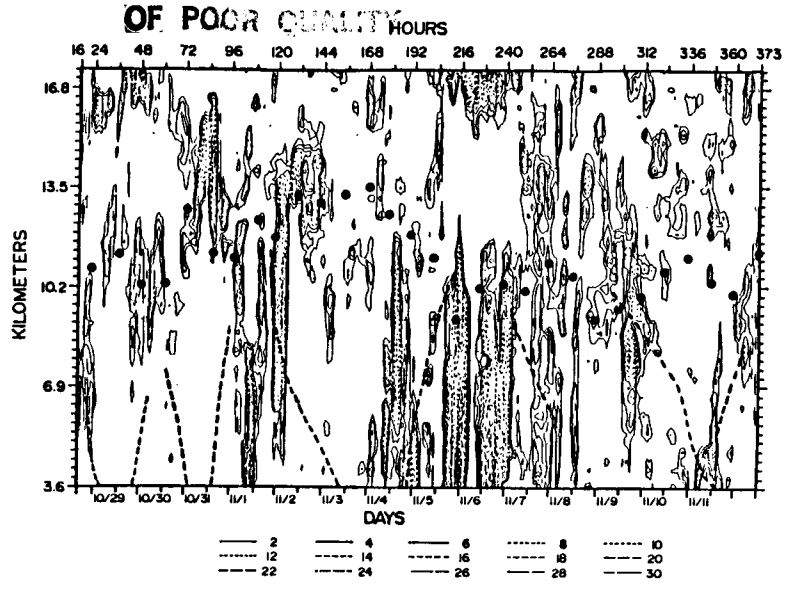

Figure 3. Upward velocity (cm/s) with hourly profiles and contours as indicated.

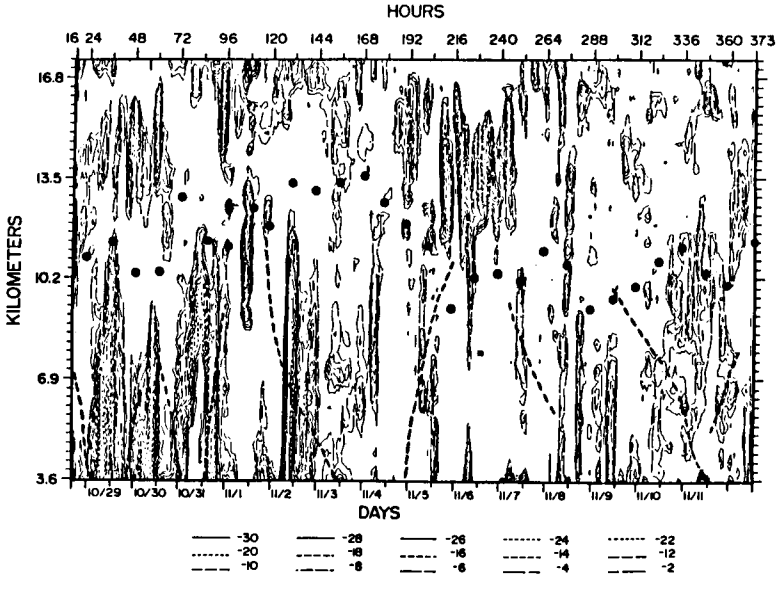

Figure 4. Downward velocity (cm/s) with hourly profiles and contours as indicated.

The occluded front is characterized by banded regions of subsiding air. There are several areas with strong downward velocity throughout the entire pocket of the occluded front at all levels of the troposphere. Two of these columns of air begin in the stratosphere around 1400 GMT and 1800 GMT on October 29. There are also cells of rising air alternating with cells of subsidence above the cold front. These cells frequently contain velocities up to 26 cm/s. The dominating downward flow in the occluded pocket, especially above the cold front, is an unexpected feature but could be caused by the complex circulation around the occluded frontal zone. The frequent intrusions of air across the tropopause is also an unexpected feature of the occlusion.

TROPOPAUSE FOLD

On November 2, the upward thrust of a column of air with wind speeds up to 16 cm/s seems to be the source of the tropopause rise. This region of rising air may be caused by the associated warm front. Immediately following this column of rising air is a strong downward flow of air which begins around 12 km just behind the warm front. This stratified region continues downward across the frontal zone where vertical wind speeds intensify up to 30 cm/s. The warm frontal zone may be the almost vertical boundary between the stratified columns of rising and subsiding air, but, when drawn in Figures 3 and 4 as derived from the reflectivity and potential temperature contours, the frontal zone appears to be located in the column of rising air at upper levels.

COLD FRONT

The cold front on November 4 and November 5 causes four or five columns of rising air, where the last two columns may be associated with the large warm front beginning on November 9 or with the upper-level front beginning on November 7. The first column arrives eight or nine hours before the cold front arrives at the surface, extends about ten or eleven hours past the surface arrival, and has upward velocities up to 12 cm/s. There are also smaller columns of rising and subsiding air on both sides of the major column.

The second column of air has stronger velocities than the first column and begins about 23 hours after the cold front begins at the surface. This column is beneath the cold frontal zone and has strong upward velocities at lower levels up to 20 cm/s and upper-level velocities of only 15 cm/s.

The third column begins about five hours after the second column ends and almost 40 hours after the surface frontal passage. Similar to the second column, the highest velocities are in the lower regions of the column. Velocities up to 20 cm/s are found in the lower levels compared to 10 cm/s in the upper levels. The upper-level warm front on November 7 extends into this column of air at about 9 km and thus influences the associated velocity patterns.

The fourth column of air begins about eight hours after the previous column ends and almost 70 hours after the initial cold front arrives at the surface. Even though the positive velocities in this region only approach 8 cm/s, the column stretches through the tropopause and into the stratosphere. The potential temperature contours in Figure 1 do not show any fluctuations caused by the passage of air through this region. The upper-level warm front extends through this column of air and may be the major influence in the vertical velocities in this region.

There are small columns of subsiding air between these columns of rising air, but none of these regions have the spatial extent of the first four columns. The downward velocities occur above and below the cold front and have velocities up to 30 cm/s in a region beneath 4 km on November 7. Unfortu-

nately, there are only 25 hours of continuous data associated with this frontal passage. Only the first column of rising air can be examined with these data.

"RAINBANDS"

With 12-minute velocity averages, the cold front on November 4 and November 5 can also be examined in more detail. The velocity data from 1500 GMT on November 4 through 1536 GMT on November 5 are graphed in Figures 5 and 6 with upward velocities and downward velocities, respectively, contoured at 2 cm/s intervals. The location of the cold front is sketched in the contours. This view of the cold front covers only the first of the five major columns of upward velocity pictured in Figure 3. The most striking feature is the banded structure of upward velocity that appears as only one column in the hourly data. The columns seem to decrease in height as the front moves through the area, but it is not clear how far beneath the front these columns extend. Areas of downward velocity are between these columns, while other downward bands extend across the front or are located beneath the front. One band of upward velocity around 1000 GMT on November 5 rises through the tropopause. Especially noticeable is the area of rising air towards the end of the data set. One region of rising air has velocities up to 35 cm/s centered around an intense cell near 10 km. Another cell of intense rising air lies below the cold front and possibly stretches across the front.

The detailed view of the cold frontal system in Figures 5 and 6 shows that even the large columns of rising air are composed of smaller, stratified regions. The vertical velocity structure around the cold front supports the rainband model shown in Figure 7 by HOBBS et al. (1980). The banded structure in Figure 3 contains a column in the warm region and columns straddling the frontal zone, as does the rainband model, but the horizontal dimensions of the columns in Figure 3 are much larger than those of the rainband model. The entire horizontal scale of the rainband structure is only about 175 km, compared to 300 km and 200 km for the first two columns of rising air for the

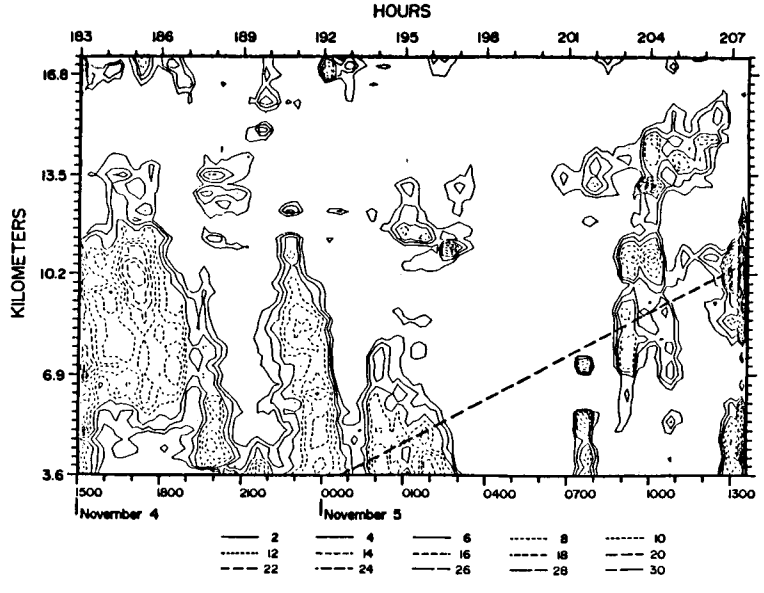

Figure 5. Upward velocity (cm/s) for the cold front with 12-minute profiles and with contours as indicated.

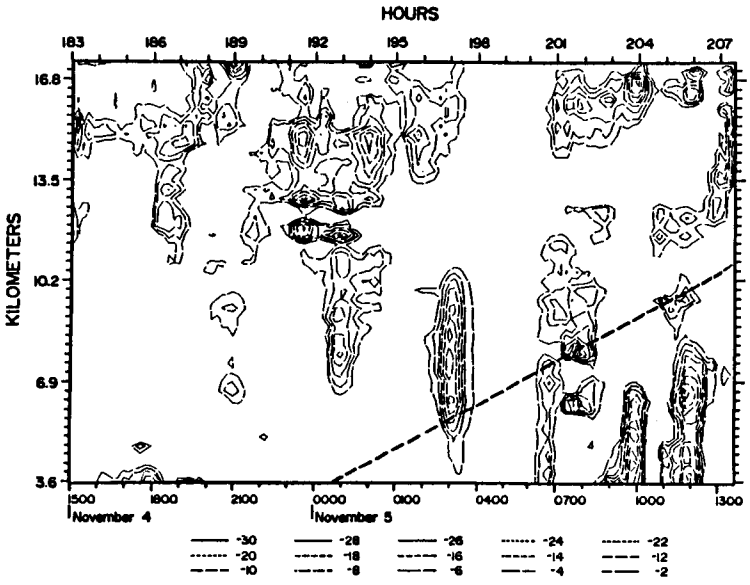

Figure 6. Downward velocity (cm/s) for the cold front with 12-minute profiles and with contours as indicated.

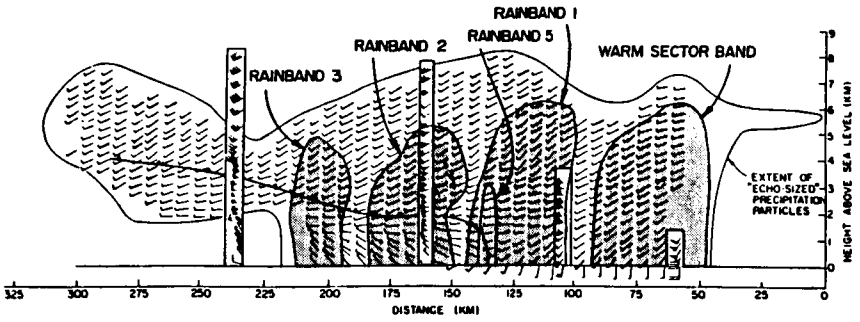

Figure 7. Rainband structure of a cross section perpendicular to a surface cold front.

analyzed cold front in Figure 3. The first column is in the warm section of the cold front in Figure 3, and stretches across the frontal zone. Since this column is also stratified into smaller columns, as seen in Figure 5, the rainbands in Figure 7 are probably associated with this region of the cold front.

The simulation of a cold front by HSIE et al. (1984) shown in Figure 8 has a vertically banded structure 600 km in front of the surface cold frontal zone and vertical bands above the frontal zone, but there are no bands stretching across the frontal zone or located beneath the zone. The vertical columns in Figures 3, 4, 5, and 6 are located in front of the surface frontal zone and behind the zone. The banded structure in Figure 8 is supported by the experimental results, but the model fails to simulate bands beneath and behind the frontal zone.

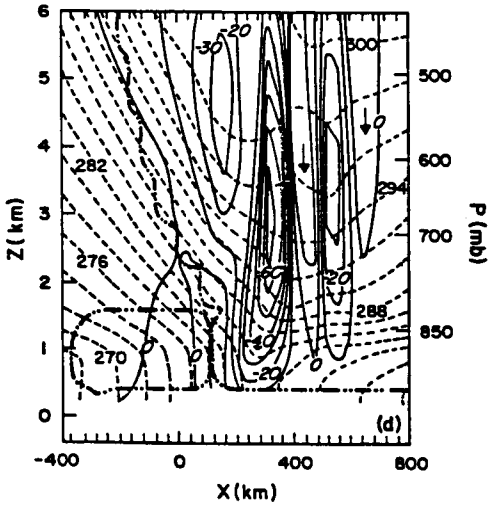

Figure 8. Cross section of the moist model of a cold front at 78 h.

WARM FRONT

The large warm front extending over November 9, 10, 11, and 12 has similar features to the other warm fronts studied in this data set. A column of rising air on November 11 is directly over a strong flow of downward velocities. The upward velocities approach 14 cm/s, but the downward velocities reach 30 cm/s. There are large areas of weak subsidence above the front, but there is a strong column of downward velocities on November 12. The upper-level cold front of November 11 also influences the velocity structure in this region, but it is not possible to determine the extent of this influence.

CONCLUSION

Vertical velocity data and reflectivity data from the SOUSY VHF radar were analyzed for a 15-day period in October and November of 1981. The analysis supports the use of the VHF radar as an effective tool for locating the tropopause and upper-level fronts and provides a detailed observation of the vertical circulation around frontal systems.

The tropopause levels recorded by the radiosonde and those calculated from the potential temperature contours and temperature contours correspond well to the levels determined from the radar reflectivities. Likewise, the frontal

systems, established from the potential temperature contours, the weather maps, and the temperature, pressure, and refractivity data, are identifiable in the reflectivity data as well. These results support the findings of LARSEN and ROTTGER (1982, 1983, 1984) on the effectiveness of the VHF radar. The analysis of the vertical velocity data reveals the stratification of rising and subsiding air columns around frontal zones. In regions of strong velocity the stratification is intensified.

Circulation patterns around the warm fronts show rising air, especially at the upper levels of the frontal zones. There is some stratification around warm fronts, but the circulation is not as strong as the velocity near the cold fronts. The overall patterns around the cold and the warm fronts were expected results. The vertical circulation associated with the two occlusions, however, contains much stronger velocities and a larger area of subsidence in the pockets than was expected. These results indicate that occluded fronts may play a more important role in mesoscale dynamics than was previously believed.

The vertical circulation pattern near the tropopause folding event consists of two vertically stratified columns of air moving in opposite directions stretching below it. There is also a region of upward velocity above the event that extends into the stratosphere. The tropopause is lifted nearly 3 km at one point during the event and is effectively displaced for over four days. Analysis of the associated potential vorticity is necessary to determine whether a tropopause folding event actually occurred.

ACKNOWLEDGEMENT

TSD and MFL were supported by the Air Force Office of Scientific Research under grant AFOSR-85-2016 while this work was carried out.

REFERENCES

Dennis, T. S. (1985), Observations of mesoscale vertical velocities around frontal zones, M.S. thesis, Department of Physics, Clemson, University.

Hobbs, P. V., T. J. Matejka, P. H. Herzegh, J. D. Locatelli, and R. A. Houze, Jr. (1980), The mesoscale and microscale structure and organization of clouds and precipitation in mid-latitude cyclones. Part I: A case study of a cold front, J. Atmos. Sci., 37, 568-596.

Hsie, E.-Y, R. A. Anthes, and D. Keyser (1984), Numerical simulation of frontogenesis in a moist atmosphere, J. Atmos. Sci., 41, 2581-2594.

Larsen, M. F., and J. Rottger (1982), VHF and UHF Doppler radars as tools for synoptic research, Bull Am. Meteorol. Soc., 63, 996-1008.

Larsen, M. F., and J. Rottger (1983), Comparison of tropopause height and frontal boundary locations based on radar and radiosonde data, Geophys. Res. Lett., 10, 325-328.

Larsen, M. F., and J. Rottger (1984), Observations of frontal zone structures with a VHF Doppler radar and radiosondes, 22nd Conf. Radar Meteorol., 489-493.